

# Effect of cone-beam computed tomography metal artefact reduction on incomplete subtle vertical root fractures

Andréa Huey Tsu Wang<sup>1</sup>, Francine Kühn Panzarella<sup>2,\*</sup>, Carlos Eduardo Fontana<sup>3</sup>,  
José Luiz Cintra Junqueira<sup>2</sup>, Carlos Eduardo da Silveira Bueno<sup>1</sup>

<sup>1</sup>Division of Endodontics, Research Institute, São Leopoldo Mandic Dental School, Campinas, Brazil

<sup>2</sup>Division of Oral Radiology, Research Institute, São Leopoldo Mandic Dental School, Campinas, Brazil

<sup>3</sup>Division of Endodontics, Centre for Health Sciences, Pontifical Catholic University of Campinas, Campinas, Brazil

## ABSTRACT

**Purpose:** This study compared the accuracy of detection of incomplete vertical root fractures (VRFs) in filled and unfilled teeth on cone-beam computed tomography images with and without a metal artefact reduction (MAR) algorithm.

**Materials and Methods:** Forty single-rooted maxillary premolars were selected and, after endodontic instrumentation, were categorized as unfilled teeth without fractures, filled teeth without fractures, unfilled teeth with fractures, or filled teeth with fractures. Each VRF was artificially created and confirmed by operative microscopy. The teeth were randomly arranged, and images were acquired with and without the MAR algorithm. The images were evaluated with OnDemand software (Cybermed Inc., Seoul, Korea). After training, 2 blinded observers each assessed the images for the presence and absence of VRFs 2 times separated by a 1-week interval. *P*-values < 0.05 were considered to indicate significance.

**Results:** Of the 4 protocols, unfilled teeth analysed with the MAR algorithm had the highest accuracy of incomplete VRF diagnosis (0.65), while unfilled teeth reviewed without MAR were associated with the least accurate diagnosis (0.55). With MAR, an unfilled tooth with an incomplete VRF was 4 times more likely to be identified as having an incomplete VRF than an unfilled tooth without this condition, while without MAR, an unfilled tooth with an incomplete VRF was 2.28 times more likely to be identified as having an incomplete VRF than an unfilled tooth without this condition.

**Conclusion:** The use of the MAR algorithm increased the diagnostic accuracy in the detection of incomplete VRF on images of unfilled teeth. (*Imaging Sci Dent* 2023; 53: 11-9)

**KEY WORDS:** Cone-Beam Computed Tomography; Tooth Root; Tooth Fractures; Artifacts

## Introduction

A vertical root fracture (VRF) is characterised by cracks or fractures on the surface of the tooth root and can be classified as complete or incomplete when the root fragments are not separated.<sup>1,2</sup> This diagnosis represents one of the most challenging tasks in dentistry, since an error can result in

unnecessary tooth extraction.<sup>3</sup>

The diagnostic accuracy of cone-beam computed tomography (CBCT) has been highlighted over the years;<sup>4,5</sup> however, if fracture lines are narrow or subtle, detection is more difficult than in the presence of separate root fragments, requiring a more experienced evaluator for an accurate diagnosis.<sup>2,6</sup>

The production of artefacts in CBCT images is associated with a decrease in diagnostic accuracy for VRFs.<sup>5,7,8</sup> High-density dental materials can produce artefacts, such as hyperdense streaks and hypodense bands; these may be superimposed on the root fracture line, preventing fracture

Received June 13, 2022; Revised October 14, 2022; Accepted October 18, 2022

Published online November 30, 2022

\*Correspondence to : Prof. Francine Kühn Panzarella

Division of Oral Radiology, Research Institute, São Leopoldo Mandic Dental School,  
Rua Dr. José Rocha Junqueira, 13 Zip code 13045-755, Campinas, São Paulo, Brazil  
(Tel) 55-19-3211-3695, E-mail) francine.panzarella@gmail.com

Copyright © 2023 by Korean Academy of Oral and Maxillofacial Radiology

This is an Open Access article distributed under the terms of the Creative Commons Attribution Non-Commercial License (<http://creativecommons.org/licenses/by-nc/3.0>) which permits unrestricted non-commercial use, distribution, and reproduction in any medium, provided the original work is properly cited.

Imaging Science in Dentistry · pISSN 2233-7822 eISSN 2233-7830

detection.<sup>9</sup>

Manufacturers of some CBCT devices have developed post-processing algorithms, such as metal artefact reduction (MAR), to minimize the effects of metal-generated artefacts.<sup>10</sup> While some studies have shown that CBCT image quality improves when a MAR algorithm is applied,<sup>10-13</sup> other research has indicated that its activation has little or no influence on the detection of root fractures<sup>14</sup> or may even hinder the diagnosis.<sup>15</sup> In addition, the use of MAR increases the time required for image reconstruction and requires more space for data storage.<sup>14</sup>

Therefore, this study was designed to compare the accuracy of the detection of incomplete root fractures of filled or unfilled teeth on CBCT images with or without MAR. The null hypothesis was that no differences would exist in the detection of incomplete root fractures of either filled or unfilled teeth based on whether the algorithm was applied.

## Materials and Methods

Approval to use extracted human teeth in this study was granted by the Ethics Committee (12792219.9.0000.5374). An *a priori* power analysis revealed a necessary minimum sample size of 40 teeth for an  $\alpha$  level of 0.05 and a desired power of 80%. The sample size calculation was performed considering a prevalence of 15% with a confidence interval of 80%.

Forty single-rooted, freshly extracted maxillary premolars with complete root formation were collected. Teeth with cracks, resorption, fractures, root canal fillings, amalgam, or crown restorations were excluded. The selected teeth were inspected with the aid of a stereoscopic magnifying glass (Tecnival SQF-F, Curitiba, PR, Brazil) of up to  $\times 40$  magnification and stored in 1% thymol to prevent drying. In total, 40 premolar teeth were included and were randomly allocated into 4 groups: unfilled teeth with MAR ( $n = 10$ ), unfilled teeth without MAR ( $n = 10$ ), filled teeth with MAR ( $n = 10$ ), and filled teeth without MAR ( $n = 10$ ).

The pulp chamber was accessed with the aid of a spherical drill (no. 1013; FAVA Indústria, São Paulo, SP, Brazil) and a frustoconical drill (no. 3071; FAVA Indústria), using a high-speed pen (Kavo do Brasil, Joinville, SC, Brazil) under refrigeration. After the pulp chamber was opened, the root canal was located with the aid of an exploratory probe. The conduit was explored with manual #10 and #15 K-files (Dentsply Maillefer, Tulsa, OK, USA). Instrumentation was performed with a reciprocating system according to the process described by Yared,<sup>16</sup> using Reciproc R25 files (VDW, Munich, Germany) with a VDW engine (VDW) in Reciproc

mode with the working length 1 mm below the apical foramen. A #10 K-file (Dentsply, Konstanz, Germany) was introduced into the root canal up to the patency (1 mm beyond the apical foramen).

The chemomechanical preparation of the root canal was performed with a 2.5% sodium hypochlorite auxiliary substance, inserted into the canal using a 5-mL hypodermic syringe (INJEX Indústrias Cirúrgicas, Ourinhos, SP, Brazil) and a 20 mm  $\times$  0.55 mm irrigation needle (INJEX Indústrias Cirúrgicas, Ourinhos, SP, Brazil) until the canal was filled. This was followed by mechanical instrumentation through the reciprocating system (Reciproc; VDW), with patency established and replacement of the auxiliary substance performed at each root third.

After preparation and modelling of the entire length of the root canal, passive ultrasonic irrigation was performed using three 20-second cycles of irrigation with 17% EDTA and three 20-second cycles of irrigation with 2.5% sodium hypochlorite, according to the process described by van der Sluis et al.<sup>17</sup> A solution of 17% EDTA (Fórmula e Ação, São Paulo, SP, Brazil) was inserted into the canal with a 5-mL hypodermic syringe (INJEX Indústrias Cirúrgicas, Ourinhos, SP, Brazil) and a 20  $\times$  0.5 irrigation needle (INJEX Indústrias Cirúrgicas, Ourinhos, SP, Brazil) to remove the smear layer. The canal was dried using a silicone cannula (Capillary Tips; Ultradent, Indaiatuba, SP, Brazil) and absorbent paper points. Endodontic instrumentation was performed, and one-half of the samples were filled with filling material. The tooth canals were filled using the modified Tagger technique, with gutta-percha cones (Tanariman Industrial Ltda, Manaus, AM, Brazil) and AH Plus cement (Dentsply, Konstanz, Germany), and manipulated according to the manufacturer's instructions.

The roots were covered with a thin layer of wax to simulate the periodontal ligament and were included in a block of self-curing acrylic resin (Jet; Artigos Odontológicos Clássico Ltda, São Paulo, SP, Brazil), positioned with the buccal and lingual markings. After the identification of each specimen, 20 roots underwent an artificial fracture procedure.

The root was fractured on a universal mechanical testing machine (DL 2000; EMIC, São José dos Pinhais, PR, Brazil). The specimen was subjected to compressive loading of a load cell of 2000 kg, with a speed of 1 mm/min, through an active tip specifically designed for such research.<sup>5</sup> This tip was introduced at the entrance of the channel, allowing the VRF to be determined using the operation cessation protocol of the machine, which is programmed to cease the emission of force when it no longer encounters resistance (Fig. 1). Teeth with visible separation of the root fragments

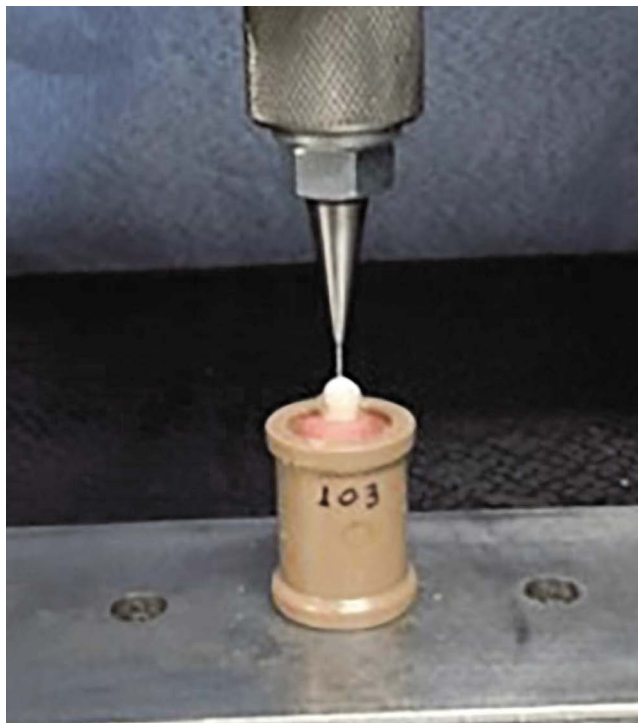


**Fig. 1.** Positioning of the specimen in the universal mechanical testing machine.

were excluded.

All teeth were inspected by direct visualisation with an operating microscope (Alliance, São Carlos, SP, Brazil) at  $\times 16$  magnification to confirm the presence, location, and position of the VRF lines, and for use as a reference standard (Fig. 2).

Images were obtained using a CBCT device (Orthopantomograph<sup>®</sup> OP300; Instrumentarium, Tuusula, Finland) in accordance with the device's maximum resolution protocol, with a voxel size of 0.086 mm and a field of view (FOV) of 5 cm  $\times$  5 cm. Subsequently, the images were exported in the Digital Imaging and Communication in Medicine (DICOM) format for evaluation of the entire volume acquired. After previous training, 2 dentists with more than 3 years of experience in CBCT independently evaluated the tomographic images produced with and without the MAR algorithm for the presence or absence of VRFs using OnDemand3D software (Cybermed Inc., Seoul, Korea) (Fig. 3). The DICOM files sent to the observers were identified with codes, to guarantee masking in relation to the type of image. Each dentist assessed the images twice, separated by a 1-week interval, in an environment with reduced light.

The sample was divided between teeth with and without filling and with and without MAR, and the data were organized as demonstrated in Table 1. The kappa coefficient

**Table 1.** Descriptions of groups and interventions performed on each tooth and image

Group	n	Interventions performed on each tooth	n	Interventions performed on each image
Unfilled teeth	10	No fracture	10	No MAR
			10	MAR
Filled teeth	10	No fracture	10	No MAR
			10	MAR
Unfilled teeth	10	Fracture	10	No MAR
			10	MAR
Filled teeth	10	Fracture	10	No MAR
			10	MAR

MAR: metal artefact reduction

was used to evaluate intraobserver and interobserver agreement, presented with the respective confidence intervals. Sensitivity, specificity, positive predictive value, negative predictive value, and positive and negative likelihood ratios were calculated to determine each evaluator's diagnostic accuracy at the 2 time points. To assess intra- and inter-rater agreement, the epiR package (R Foundation for Statistical Computing, Vienna, Austria) was used, and to assess whether a change in diagnostic accuracy existed between assessments 1 and 2 of each observer, the McNemar test ( $P < 0.05$ ) and DTComPair package (R Core Team and the R Foundation for Statistical Computing, Auckland, New Zealand) were used. Both packages are implemented in R software version 4.2 (R Core Team and the R Foundation for Statistical Computing) for Mac iOS.

All images were reassessed after 7 days, and all variables were analysed to calculate the intra-observer and inter-observer agreement via kappa testing. For interpretation, the following reference ranges were used:  $< 0.00$ , poor; 0.00 to 0.20, slight; 0.21 to 0.40, fair; 0.41 to 0.60, moderate; 0.61 to 0.80, substantial; and  $> 0.80$ , almost perfect agreement, in accordance with Landis and Koch.<sup>18</sup>

## Results

In this sample, 40% of incomplete VRFs were detected on the palatal surface, 30% on the buccal surface, 20% on the mesial surface, and 10% involving the buccal and palatal surfaces. Exactly 50% affected the cervical and middle thirds of the root, 18.18% affected the entire root extension, and 13.63% affected the middle and apical thirds. In the remaining cases (18.19%), the VRF affected only 1 root

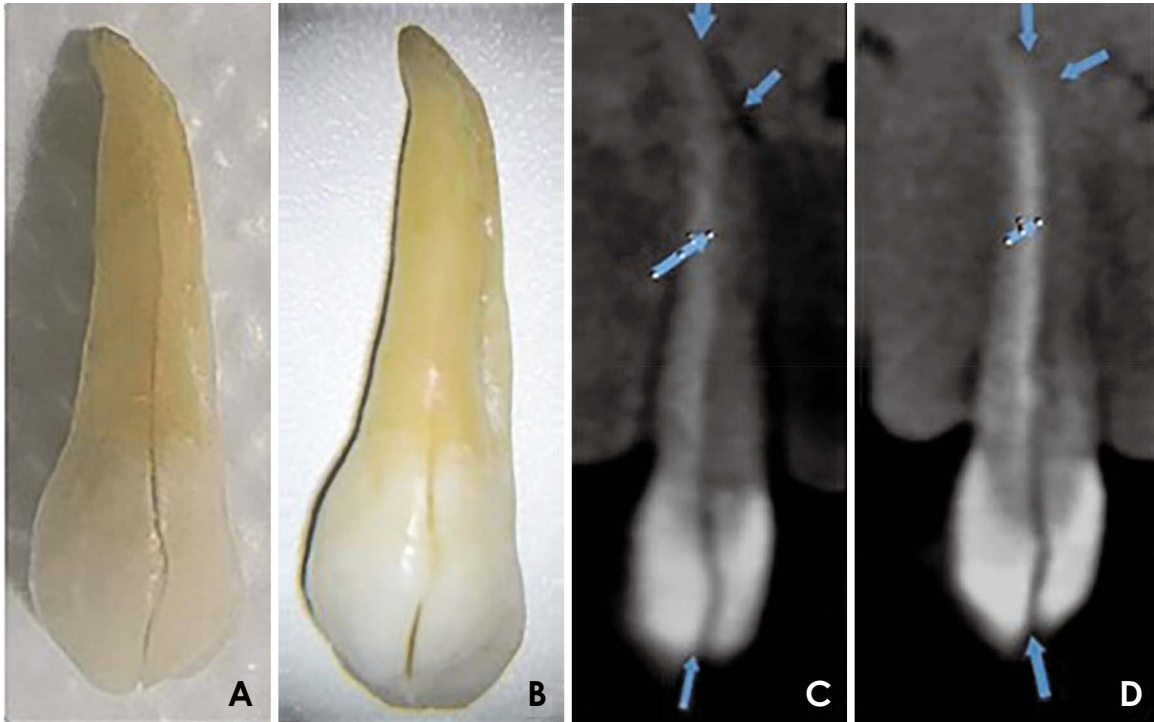


**Fig. 2.** A. Clinical image. B. Image taken using a microscope. C. Cone-beam computed tomographic (CBCT) image without metal artefact reduction (MAR). D. CBCT image with MAR of the dental element with incomplete vertical root fracture. For images C and D, the arrows indicate the fracture line.

**Table 2.** Interobserver agreement for each group

	Accuracy	Interobserver kappa	Confidence interval (95%)
Unfilled teeth with MAR	0.65	1.00	0.56-1.44
Unfilled teeth without MAR	0.55	1.00	0.56-1.46
Filled teeth with MAR	0.60	1.00	0.56-1.46
Filled teeth without MAR	0.65	0.79	0.35-1.23

MAR: metal artefact reduction

third (either the cervical, middle, or apical third).

Of the 4 protocols, unfilled teeth analysed with the MAR algorithm were associated with the most accurate diagnosis of incomplete VRF (0.65), while unfilled teeth without MAR were associated with the least accurate diagnosis (0.55) (Table 2). Although filled teeth analysed without MAR received the same accuracy score as unfilled teeth with MAR (0.65) (Table 2), the associated interobserver coefficient (0.79) was the lowest among the 4 protocols (Table 2).

For both evaluators, unfilled teeth assessed with MAR had the highest specificity values (0.90; range, 0.71 to 1.00) of the protocols. For that group, a statistically significant difference was found between the first and second assess-

ments, with  $P$ -values of  $P=0.025$  and  $P=0.014$ , respectively, by applying the McNemar test ( $P<0.05$ ).

The kappa coefficient for agreement between the 2 assessments of each examiner was high, ranging from 0.88 to 1.00. While the interobserver agreement was excellent overall, the lowest agreement (kappa of 0.79) was observed for filled teeth without MAR, as shown in Table 2.

The probability that unfilled teeth identified as having an incomplete VRF actually exhibited this condition was 80% with MAR and 62% without MAR, whereas the probability that unfilled teeth identified as not having an incomplete VRF did not exhibit the condition was 60% with MAR and 64% without MAR (Table 3). With MAR, an unfilled tooth with an incomplete VRF was 4 times more likely to be iden-

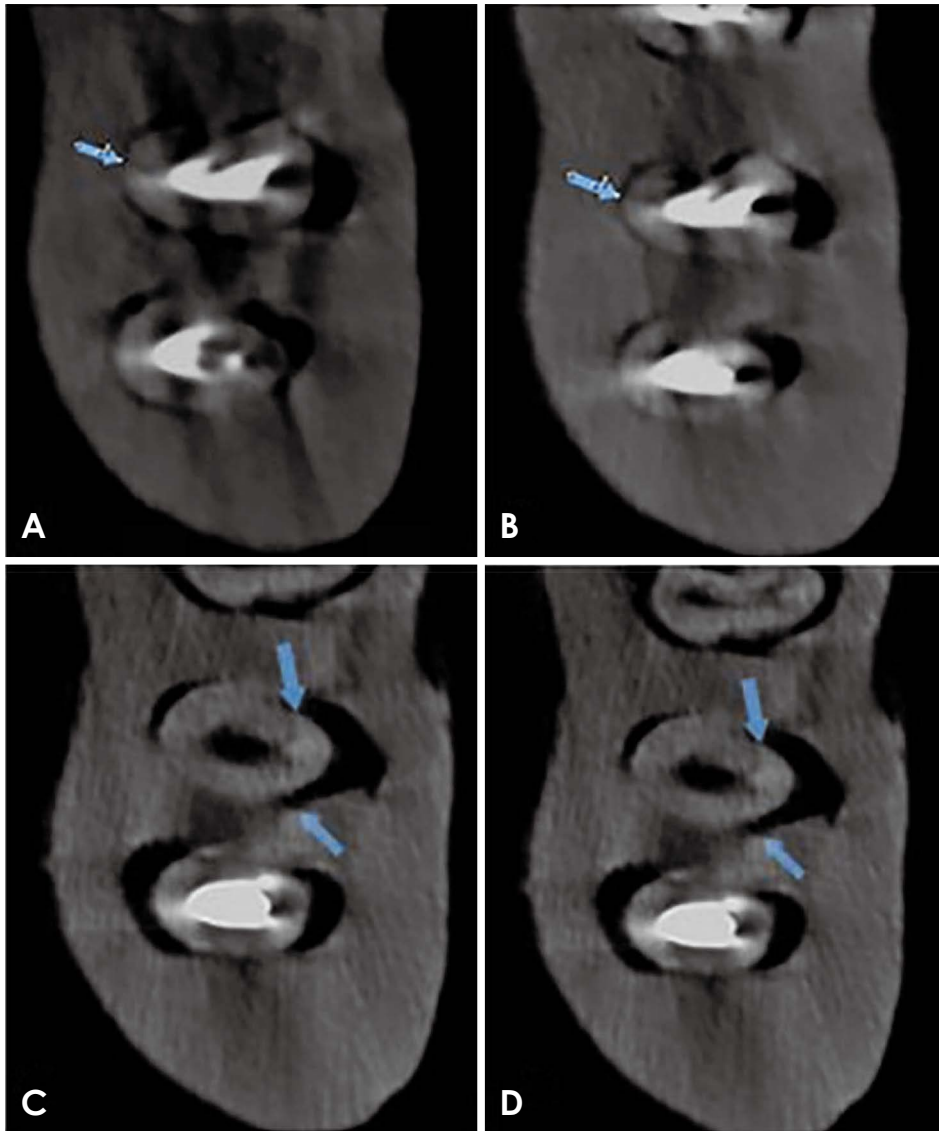


**Fig. 3.** A. Axial images of a filled tooth without metal artefact reduction (MAR). B. Axial images of a filled tooth with MAR. C. Axial images of an unfilled tooth without MAR. D. Axial images of an unfilled tooth with MAR. The arrows illustrate an incomplete fracture line. Note the hypodense bands emanating from the filling material of the canal. MAR: metal artefact reduction.

**Table 3.** Diagnostic tests for incomplete vertical root fracture detection in unfilled teeth with and without metal artefact reduction (MAR) overall and by observer

	Sensitivity	Specificity	PPV	NPV	LR+	LR-
Overall						
With MAR	0.4	0.90	0.80	0.60	4.00	0.67
Without MAR	0.8	0.65	0.62	0.64	2.28	0.31
Observer 1						
With MAR	0.40	0.90	0.80	0.60	4.00	0.67
Without MAR	0.80	0.70	0.57	0.54	1.33	0.87
Observer 2						
With MAR	0.40	0.90	0.80	0.60	4.00	0.67
Without MAR	0.80	0.60	0.67	0.75	2.00	0.33

PPV: positive predictive value, NPV: negative predictive value, LR+ : positive likelihood ratio, LR-: negative likelihood ratio

**Table 4.** Diagnostic tests for incomplete vertical root fracture detection in filled teeth with and without metal artefact reduction (MAR) overall and by observer

	Sensitivity	Specificity	PPV	NPV	LR+	LR-
Overall						
With MAR	0.55	0.65	0.39	0.37	1.57	0.69
Without MAR	0.60	0.70	0.67	0.64	2.00	0.57
Observer 1						
With MAR	0.60	0.60	0.16	0.16	1.5	0.67
Without MAR	0.60	0.70	0.67	0.64	2.00	0.57
Observer 2						
With MAR	0.50	0.70	0.62	0.58	1.67	0.71
Without MAR	0.60	0.70	0.67	0.64	2.00	0.57

PPV: positive predictive value, NPV: negative predictive value, LR+: positive likelihood ratio, LR-: negative likelihood ratio

tified as having an incomplete VRF than an unfilled tooth without this condition, and without MAR, an unfilled tooth with an incomplete VRF was 2.28 times more likely to be identified as having an incomplete VRF than an unfilled tooth without this condition (Table 3).

The probability that filled teeth identified as having an incomplete VRF did have this condition was 39% with MAR and 67% without MAR, whereas the probability that filled teeth identified as not having an incomplete VRF did not have the condition was 37% with MAR and 64% without MAR (Table 4). With MAR, a filled tooth with an incomplete VRF was 1.57 times more likely to be identified as having an incomplete VRF than a filled tooth without this condition, and without MAR, a filled tooth with an incomplete VRF was 2 times more likely to be identified as having an incomplete VRF than a filled tooth without the condition (Table 4).

## Discussion

Endodontic sealer and gutta-percha cones contain radiopacifiers such as zinc oxide and barium sulphate,<sup>19</sup> which are high-density materials that produce artefacts in tomographic images, potentially impairing image quality. These effects can be minimised by activating the MAR algorithm.<sup>11,20</sup> The present results indicate that the use of the MAR algorithm in unfilled teeth improved the diagnosis rate of incomplete VRF, in accordance with several previous studies.<sup>1,6,8,21,22</sup>

Considerable variation currently exists among the findings on the influence of the MAR algorithm in the diagnosis of fractures. Bechara et al.<sup>13</sup> observed that the use of MAR decreased the accuracy of detection of VRFs in endodon-

tically treated teeth. In contrast, several studies<sup>4,15,23-25</sup> showed no significant difference, while others reported that MAR was more effective when the object of the image was in the centre of the FOV than otherwise.<sup>11,26</sup> These differences may relate to the methodology used to obtain the root fractures, the width between the root fragments<sup>6,27</sup> or the absence of acquisition protocols with high resolution,<sup>28</sup> which may have affected the detectability of root fractures on CBCT.

So far, few studies have been conducted to evaluate incomplete root fractures.<sup>29</sup> Since an incomplete root fracture originates from the root,<sup>30</sup> a tip was developed for use in a universal testing machine to obtain precise control of the force applied to the roots. The methodology used in the present study to create the root fracture was similar to that used in previous studies.<sup>8,31,32</sup> Operative microscopy was used to detect the presence or absence of a root fracture, as in the study by Yuan et al.,<sup>33</sup> and was noteworthy for its non-destructive nature.

In the present study, among the fractured teeth, 50% of the fracture lines were found in the cervical and middle thirds of the root, 18.18% in the entire root extension, 13.63% in the middle and apical thirds, and 18.19% in only 1 of the root thirds (the cervical, middle, or apical third). Regarding the root surface, the fracture line involved the palatal aspect in 40% of the cases, the buccal aspect in 30%, the mesial aspect in 20%, and the buccal and palatal aspects in 10%. This differs from complete fractures, which normally extend in the vestibulolingual dimension.<sup>28,34</sup> *In vivo* studies have shown that early root fracture lines can be quite subtle.<sup>6,35,36</sup> The lack of studies exclusively focused on incomplete fractures, as well as the *in vitro* nature of the present study, limits the results available for comparison.



The sensitivity and specificity values in this sample decreased in the presence of fracture. Hassan et al.<sup>32</sup> concluded that the presence of gutta-percha did not influence the sensitivity of CBCT images, although it reduced the specificity. According to Marinho Vieira et al.,<sup>22</sup> teeth with gutta-percha displayed the highest artefact interference of the groups studied, disfavoured the detection of root fractures. Oliveira et al.<sup>15</sup> evaluated the performance of the MAR algorithm with a methodology similar to that used in this study and found that all measures of diagnostic accuracy decreased when MAR was applied. However, those authors did not report which teeth had incomplete fractures and which were joined after the root fragments had been separated.

Both intra- and inter-examiner agreement were high in this study, as the assessments were conducted after the examiners were trained. Problems with concordance have been reported in previous studies.<sup>27,37-39</sup> In one of these,<sup>6</sup> fewer than one-third of subtle fractures were detected by experienced radiologists, signalling the subjective nature of the interpretation of CBCT images. This finding highlights the need for improvement and constant training for those who interpret CBCT images.<sup>40</sup>

In some studies, researchers have attributed the relatively weak agreement between examiners to the difficulty of identifying the VRF due to the tomography unit used, the orientation of the fracture line, and the presence of intracanal materials.<sup>4</sup> According to a recent study, the OP300 device, which was used to obtain the images in the present study, exhibits good accuracy in the detection of VRFs.<sup>41</sup> Removing root canal materials prior to imaging could improve the diagnostic potential of CBCT,<sup>21</sup> but this is not a viable practice considering the patient's perspective. Diagnostic accuracy for subtle VRFs can be improved by using a high-resolution acquisition protocol<sup>4,27</sup> with increased exposure time and a small FOV.<sup>6</sup>

Some limitations of the present research should be considered. First, many *ex vivo* studies have already been carried out.<sup>1,21,22,36,42,43</sup> Due to the laboratorial design of the current study, the signs and symptoms of the condition studied are not reproduced. Pain on percussion, localized periodontal pocket, and tooth mobility are associated with the presence of advanced root fractures.<sup>4</sup> Bucco/buccolingual bone loss was reported as an important indirect sign<sup>29,36</sup> and should be considered in the diagnostic evaluation even when the fracture line cannot be visualized, with periodontal exploration or surgical extraction as confirmatory procedures.<sup>4</sup>

Also, the lack of information on the prevalence of incomplete VRF in the population may have influenced the sam-

ple calculation. The prevalence of incomplete VRF is not clearly established; rates ranging from 11% to 20% have been found, and some studies have shown values as high as 31.7%.<sup>31</sup> This variation is justified by the different methodologies used in the studies, factors related to data acquisition, and incorrect or imprecise diagnosis. In a recent study<sup>15</sup> with a similar methodology to the present one, 45 teeth were used, which reinforces the confidence in the sample calculation.

A significant reduction has been observed in the diagnostic capacity of CBCT when the root fragments are less than 0.5 mm apart.<sup>3,39</sup> In the present study, the distance between the fragments on the root surface could not be evaluated; however, future studies could incorporate evaluation of this measure by associating the location and direction of the fracture line.

In conclusion, the presence of filling material along with the use of an MAR influences the success of incomplete VRF detection. The width between the root fragments and the absence of high-resolution acquisition protocols may have affected the detectability of root fractures on CBCT.

**Conflicts of Interest:** None

## References

1. Neves FS, Freitas DQ, Campos PS, Ekstubb A, Lofthag-Hansen S. Evaluation of cone-beam computed tomography in the diagnosis of vertical root fractures: the influence of imaging modes and root canal materials. *J Endod* 2014; 40: 1530-6.
2. Gao A, Cao D, Lin Z. Diagnosis of cracked teeth using cone-beam computed tomography: literature review and clinical experience. *Dentomaxillofac Radiol* 2021; 50: 20200407.
3. Özer SY. Detection of vertical root fractures of different thicknesses in endodontically enlarged teeth by cone beam computed tomography versus digital radiography. *J Endod* 2010; 36: 1245-9.
4. De Martin E Silva D, Campos CN, Pires Carvalho AC, Devito KL. Diagnosis of mesiodistal vertical root fractures in teeth with metal posts: influence of applying filters in cone-beam computed tomography images at different resolutions. *J Endod* 2018; 44: 470-74.
5. Dias DR, Iwaki LC, de Oliveira AC, Martinhão FS, Rossi RM, Araújo MG, et al. Accuracy of high-resolution small-volume cone-beam computed tomography in the diagnosis of vertical root fracture: an in vivo analysis. *J Endod* 2020; 46: 1059-66.
6. Gulibire A, Cao Y, Gao A, Wang C, Wang T, Xie X, et al. Assessment of true vertical root fracture line in endodontically treated teeth using a new subtraction software - a micro-CT and CBCT study. *Aust Endod J* 2021; 47: 290-7.
7. Aristizabal-Elejalde D, Arriola-Guillén LE, Aliaga-Del Castillo A, Ruíz-Mora GA, Rodríguez-Cárdenas YA. Assessment of fractures in endodontically treated teeth restored with and without

- root canal posts using high-resolution cone beam computed tomography. *J Clin Exp Dent* 2020; 12: e547-54.
8. Khedmat S, Rouhi N, Drage N, Shokouhinejad N, Nekoofar MH. Evaluation of three imaging techniques for the detection of vertical root fractures in the absence and presence of gutta-percha root fillings. *Int Endod J* 2012; 45: 1004-9.
  9. Coelho-Silva F, Martins LA, Braga DA, Zandonade E, Haiter-Neto F, de-Azevedo-Vaz SL. Influence of windowing and metal artefact reduction algorithms on the volumetric dimensions of five different high-density materials: a cone-beam CT study. *Dentomaxillofac Radiol* 2020; 49: 20200039.
  10. Queiroz PM, Santaella GM, Groppo FC, Freitas DQ. Metal artifact production and reduction in CBCT with different numbers of basis images. *Imaging Sci Dent* 2018; 48: 41-4.
  11. Queiroz PM, Groppo FC, Oliveira ML, Haiter-Neto F, Freitas DQ. Evaluation of the efficacy of a metal artifact reduction algorithm in different cone beam computed tomography scanning parameters. *Oral Surg Oral Med Oral Pathol Oral Radiol* 2017; 123: 729-34.
  12. Freitas DQ, Fontenele RC, Nascimento EH, Vasconcelos TV, Noujeim M. Influence of acquisition parameters on the magnitude of cone beam computed tomography artifacts. *Dentomaxillofac Radiol* 2018; 47: 20180151.
  13. Bechara B, Moore WS, McMahan CA, Noujeim M. Metal artefact reduction with cone beam CT: an in vitro study. *Dentomaxillofac Radiol* 2012; 41: 248-53.
  14. Fontenele RC, Nascimento EH, Santaella GM, Freitas DQ. Does the metal artifact reduction algorithm activation mode influence the magnitude of artifacts in CBCT images? *Imaging Sci Dent* 2020; 50: 23-30.
  15. Oliveira MR, Sousa TO, Caetano AF, de Paiva RR, Valladares-Neto J, Yamamoto-Silva FP, et al. Influence of CBCT metal artifact reduction on vertical radicular fracture detection. *Imaging Sci Dent* 2021; 51: 55-62.
  16. Yared G. Canal preparation using only one Ni-Ti rotary instrument: preliminary observations. *Int Endod J* 2008; 41: 339-44.
  17. van der Sluis LW, Vogels MP, Verhaagen B, Macedo R, Wesselink PR. Study on the influence of refreshment/activation cycles and irrigants on mechanical cleaning efficiency during ultrasonic activation of the irrigant. *J Endod* 2010; 36: 737-40.
  18. Landis JR, Koch GG. The measurement of observer agreement for categorical data. *Biometrics* 1977; 33: 159-74.
  19. Makins SR. Artifacts interfering with interpretation of cone beam computed tomography images. *Dent Clin North Am* 2014; 58: 485-95.
  20. Helvacioğlu-Yigit D, Demirturk Kocasarac H, Bechara B, Noujeim M. Evaluation and reduction of artifacts generated by 4 different root-end filling materials by using multiple cone-beam computed tomography imaging settings. *J Endod* 2016; 42: 307-14.
  21. Hekmatian E, Karbasi Kheir M, Fathollahzade H, Sheikhi M. Detection of vertical root fractures using cone-beam computed tomography in the presence and absence of gutta-percha. *ScientificWorldJournal* 2018; 2018: 1920946.
  22. Marinho Vieira LE, Diniz de Lima E, Peixoto LR, Oliveira Pinto MG, Sousa Melo SL, Oliveira ML, et al. Assessment of the influence of different intracanal materials on the detection of root fracture in bicrooked teeth by cone-beam computed tomography. *J Endod* 2020; 46: 264-70.
  23. Dalili Kajan Z, Taramsari M, Khosravi Fard N, Khaksari F, Moghasem Hamidi F. The efficacy of metal artifact reduction mode in cone-beam computed tomography images on diagnostic accuracy of root fractures in teeth with intracanal posts. *Iran Endod J* 2018; 13: 47-53.
  24. Koç C, Kamburoğlu K, Sönmez G, Yılmaz F, Gülen O, Karahan S. Ability to detect endodontic complications using three different cone beam computed tomography units with and without artefact reduction modes: an ex vivo study. *Int Endod J* 2019; 52: 725-36.
  25. Ferreira LM, Visconti MA, Nascimento HA, Dallemolle RR, Ambrosano GM, Freitas DQ. Influence of CBCT enhancement filters on diagnosis of vertical root fractures: a simulation study in endodontically treated teeth with and without intracanal posts. *Dentomaxillofac Radiol* 2015; 44: 20140352.
  26. Nikbin A, Dalili Kajan Z, Taramsari M, Khosravifard N. Effect of object position in the field of view and application of a metal artifact reduction algorithm on the detection of vertical root fractures on cone-beam computed tomography scans: an in vitro study. *Imaging Sci Dent* 2018; 48: 245-54.
  27. Guo XL, Li G, Zheng JQ, Ma RH, Liu FC, Yuan FS, et al. Accuracy of detecting vertical root fractures in non-root filled teeth using cone beam computed tomography: effect of voxel size and fracture width. *Int Endod J* 2019; 52: 887-98.
  28. Wanderley VA, Neves FS, Nascimento MC, Monteiro GQ, Lobo NS, Oliveira ML, et al. Detection of incomplete root fractures in endodontically treated teeth using different high-resolution cone-beam computed tomographic imaging protocols. *J Endod* 2017; 43: 1720-4.
  29. Zhang L, Wang T, Cao Y, Wang C, Tan B, Tang X, et al. In vivo detection of subtle vertical root fracture in endodontically treated teeth by cone-beam computed tomography. *J Endod* 2019; 45: 856-62.
  30. Rivera EM, Walton RE. Longitudinal tooth fractures: findings that contribute to complex endodontic diagnoses. *Endod Topics* 2007; 16: 82-111.
  31. Tsesis I, Rosen E, Tamse A, Taschieri S, Kfir A. Diagnosis of vertical root fractures in endodontically treated teeth based on clinical and radiographic indices: a systematic review. *J Endod* 2010; 36: 1455-8.
  32. Hassan B, Metska ME, Ozok AR, van der Stelt P, Wesselink PR. Detection of vertical root fractures in endodontically treated teeth by a cone beam computed tomography scan. *J Endod* 2009; 35: 719-22.
  33. Yuan M, Gao AT, Wang TM, Liang JH, Aihemati GB, Cao Y, et al. Using meglumine diatrizoate to improve the accuracy of diagnosis of cracked teeth on cone-beam CT images. *Int Endod J* 2020; 53: 709-14.
  34. Kapralos V, Koutroulis A, Irinakakis E, Kouros P, Lyroudia K, Pitas I, et al. Digital subtraction radiography in detection of vertical root fractures: accuracy evaluation for root canal filling, fracture orientation and width variables. An ex-vivo study. *Clin Oral Investig* 2020; 24: 3671-81.
  35. Özer SY. Detection of vertical root fractures by using cone beam computed tomography with variable voxel sizes in an in vitro model. *J Endod* 2011; 37: 75-9.
  36. Byakova SF, Novozhilova NE, Makeeva IM, Grachev VI, Kasat-



- kina IV. The detection of vertical root fractures in post-core restored teeth with cone-beam CT: in vivo and ex vivo. *Dentomaxillofac Radiol* 2019; 48: 20180327.
37. Freitas-E-Silva A, Mármora B, Barriviera M, Panzarella FK, Raitz R. CBCT performance and endodontic sealer influence in the diagnosis of vertical root fractures. *J Contemp Dent Pract* 2019; 20: 552-6.
  38. Chavda R, Mannocci F, Andiappan M, Patel S. Comparing the in vivo diagnostic accuracy of digital periapical radiography with cone-beam computed tomography for the detection of vertical root fracture. *J Endod* 2014; 40: 1524-9.
  39. Brady E, Mannocci F, Brown J, Wilson R, Patel S. A comparison of cone beam computed tomography and periapical radiography for the detection of vertical root fractures in nonendodontically treated teeth. *Int Endod J* 2014; 47: 735-46.
  40. Patel S, Brown J, Pimentel T, Kelly RD, Abella F, Durack C. Cone beam computed tomography in endodontics - a review of the literature. *Int Endod J* 2019; 52: 1138-52.
  41. Caetano AP, Sousa TO, Oliveira MR, Evangelista K, Bueno JM, Silva MA. Accuracy of three cone-beam CT devices and two software systems in the detection of vertical root fractures. *Dentomaxillofac Radiol* 2021; 50: 20200334.
  42. Fox A, Basrani B, Lam EW. The performance of a zirconium-based root filling material with artifact reduction properties in the detection of artificially induced root fractures using cone-beam computed tomographic imaging. *J Endod* 2018; 44: 828-33.
  43. Diniz de Lima E, Lira de Farias Freitas AP, Mariz Suassuna FC, Sousa Melo SL, Bento PM, Pita de Melo D. Assessment of cone-beam computed tomographic artifacts from different intracanal materials on bicrooked teeth. *J Endod* 2019; 45: 209-13.e2.